New Phytologist

Research

A core microbiome in the hyphosphere of arbuscular mycorrhizal fungi has functional significance in organic phosphorus mineralization

Letian Wang[1]*, Lin Zhang[1]*, Timothy S. George[2] and Gu Feng[1]

[1]College of Resources and Environmental Sciences, National Academy of Agriculture Green Development, China Agricultural University, Beijing 100193, China; [2]The James Hutton Institute, Invergowrie, Dundee, DD2 5DA, UK

Author for correspondence:
Gu Feng
Email: fenggu@cau.edu.cn

Received: *3 July 2022*
Accepted: *18 November 2022*

New Phytologist (2023) **238:** 859–873
doi: 10.1111/nph.18642

Key words: arbuscular mycorrhizal fungi, co-occurrence network, core microbiome, hyphosphere, phosphorus (P).

Summary

- The mycorrhizal pathway is an important phosphorus (P) uptake pathway for more than two-thirds of land plants. The arbuscular mycorrhizal (AM) fungi-associated hyphosphere microbiome has been considered as the second genome of mycorrhizal P uptake pathway and functionality in mobilizing soil organic P (Po). However, whether there is a core microbiome in the hyphosphere and how this is implicated in mining soil Po are less understood.
- We established on-site field trials located in humid, semiarid, and arid zones and a microcosm experiment in a glasshouse with specific AM fungi and varying soil types to answer the above questions.
- The hyphosphere microbiome of AM fungi enhanced soil phosphatase activity and promoted Po mineralization in all sites. Although the assemblage of hyphosphere microbiomes identified in three climate zones was mediated by environmental factors, we detected a core set in three sites and the subsequent microcosm experiment. The core members were co-enriched in the hyphosphere and dominated by Alphaproteobacteria, Actinobacteria, and Gammaproteobacteria. Moreover, these core bacterial members aggregate into stable guilds that contributed to phosphatase activity.
- The core hyphosphere microbiome is taxonomically conserved and provides functions, with respect to the mineralization of Po, that AM fungi lack.

Introduction

Fungi are ubiquitous in terrestrial ecosystems and colonize the roots of the majority of plant species (Mommer *et al.*, 2018). They produce a massive hyphal network in the soil, known as a mycelium (Duran *et al.*, 2018). The surface of hyphae in soil is 'hot spots' for bacterial activity and is where a range of complicated fungal–bacterial interactions occur (de Boer *et al.*, 2005). Fungal exudates are the major or exclusive source of carbon (C) for their associated bacteria, and the bacteria can mobilize and supply a portion of nutrients to the fungi (de Boer *et al.*, 2005; de Menezes *et al.*, 2017). Fungi–bacteria interactions constitute a complex network and are significant drivers of diverse ecosystem functions (Deveau *et al.*, 2018). Therefore, selecting a proper research model is essential to reveal the mechanisms of this cross-kingdom interaction.

Arbuscular mycorrhizal (AM) fungi are ubiquitous in nature and agriculture ecosystems and play vital roles in plant growth by improving nutrient acquisition and enhancing tolerance of biotic and abiotic stress (Zhang *et al.*, 2019; Genre *et al.*, 2020). Arbuscular mycorrhizal fungi have been widely recognized as model organisms for ecological research because of their widespread occurrence, key ecosystem service provision, and special interactions with plant and soil microbes (Johnson & Omland, 2004; Duplessis *et al.*, 2011; Kiers *et al.*, 2011). It is noteworthy that AM fungal extraradical hyphae recruit distinct bacteria (i.e. hyphosphere microbiome) in their hyphosphere by releasing C, in return bacteria provide enhanced nutrient mobilization and turnover (L. Zhang *et al.*, 2022). Arbuscular mycorrhizal fungi are largely devoid of enzymes to release nutrients from soil organic forms, which implies a reliance on bacteria for the release of essential mineral nutrients from complex organic forms might be a compensation (Tisserant *et al.*, 2013; Sun *et al.*, 2019). Interestingly, in microcosm and *in vitro* culture conditions where AM fungal species were manipulated, fructose secreted by hyphae was suggested to serve as a signal or energy source to increase the phosphatase activity released by bacteria (Zhang *et al.*, 2018a,b). While under field conditions, diverse AM fungi have been shown to colonize crop roots simultaneously, and the extraradical hyphae recruit complex and specific bacterial communities, which create an impressively complex interaction network (Agnolucci *et al.*, 2015; Iffis *et al.*, 2016). Considering this complex

*These authors contributed equally to this work.

network of multiple interacting AM fungi and bacteria, recent research has often focused solely on hyphosphere bacterial community composition, with little consideration for their potential interactions yet (Zhang *et al.*, 2018b).

Deciphering the AM fungal–bacterial interactions in the field is a daunting task given the complex networks, and the dependence of those interactions on environmental conditions. It has been suggested that AM fungal taxa may recruit different hyphosphere bacteria through variation in the composition of their exudates (Zhou *et al.*, 2020). Host plant quality and species can affect the AM fungal communities via preferentially allocating C to higher quality partners, which may lead to variation in the hyphosphere bacterial communities (Engelmoer & Kiers, 2015; Knegt *et al.*, 2016). Varying environmental factors also play a role, with soil properties such as pH and nutrient forms, and their spatial heterogeneity influencing the AM fungal–bacterial associations (Singh *et al.*, 2008; Wang *et al.*, 2019; Emmett *et al.*, 2021). In this context, identifying a core hyphosphere microbiome may assist in the detailed understanding of these arcane (many AM fungi interacting with many bacteria) interactions. In a mesocosm experiment under glasshouse conditions, Emmett *et al.* (2021) detected a core component in the hyphosphere, which were conserved and reproducible across AM fungal species and soil types. Therefore, similar to gut and plant microbiome, we suggest that core hyphosphere microbiomes are prevalent components across complex AM fungal consortia and multiple environmental factors, especially if they are tightly linked to AM fungal functions (Neu *et al.*, 2021). However, this has yet to be explicitly tested in an agricultural setting.

To date, one-to-one (one AM fungal species to one bacterial species) experiments have provided us with detailed information about specific AM fungal–microorganism interactions, but they oversimplify complex AM fungal–bacterial systems (Salvioli *et al.*, 2016; Vannini *et al.*, 2016; Zhang *et al.*, 2018a). Moving forward, we extended the scope of the AM fungal–bacterial interactions to the many to many systems (many bacteria colonizing the hyphae of many AM fungi) through investigation of the complex AM fungal communities and hyphosphere bacterial communities *in situ* in the field. Here, we aim to assess co-occurrence patterns of complex interactions between AM fungi and hyphosphere bacteria, and the potential role of their interactions on soil nutrient cycling across three experimental sites, corresponding to contrasting soil types and climate zones in China. We hypothesized that: (1) Hyphosphere bacterial communities vary across climate zones/soil types and AM fungal communities; and (2) Hyphosphere bacterial communities contain a core microbiome associated with greater phosphatase activity and organic phosphorus (Po) mineralization.

Materials and Methods

Experiment 1: Field experiment

To characterize the hyphosphere bacterial communities and assess complicated AM fungal–bacterial interactions in the field, we selected three long-term soil fertility experiments at Hunan (HN, 11°52′E, 26°45′N), Shaanxi (SX, 108°00′E, 34°17′N), and Xinjiang (XJ, 87°46′E, 43°95′N) Provinces (Supporting Information Fig. S1a), which represented wet, semiarid, and arid environmental conditions, respectively. These three experimental sites belonged to The National Long-term Monitoring Network of Soil Fertility and Fertilizer Effects, which was founded in 1990. These experimental sites covered three typical soil types found in China (Table S1). In 2018, the crop plant was maize at the HN and SX sites, and cotton at the XJ site.

We made two types of AM fungal hyphae in-growth tubes out of polyvinyl chloride (PVC) tubes (12 cm in diameter, 5 cm in length), which were sealed with 30 μm nylon mesh (permitting AM fungal hyphae but not roots to grow into) or 0.45 μm poly tetra fluoro ethylene membrane (excluding AM fungal hyphae and roots to grow into) on the two ends, respectively (Fig. S1b, c). They also included buffer zones, which consisted of a circular PVC plate (12 cm in diameter, 1 cm in width) with many holes (1 cm in diameter) and the 30 or 0.45 μm mesh glued on both sides, which can exclude the interference of roots via the air gap (Fig. S1c). We imbedded the sterilized membranes with 0.45 μm pores (10 cm in diameter, Poly tetra fluoro ethylene, Shanghaixinya) in each in-growth tube to collect the hyphae (Methods S1; Fig. S1c). The principle is that the AM fungal hyphae enter the tube, and after encountering the membrane, the hyphae can be enriched near the membrane, which is convenient for collection. All in-growth tubes were buried to a depth of either 20 or 30 cm in soil 15 cm away from a plant at the beginning of sowing in 2018 (Fig. S1b). Each location had eight repeats of two types of in-growth tubes, and each repeat included two technical replicates. At harvest, two technical replicates were mixed into one sample for subsequent analysis. The in-growth tubes were filled with the soil, which was collected in advance from each site described above (Table S1).

Experiment 2: The microcosm experiment

This experiment was conducted to verify results found from Experiment 1 under controlled conditions. Four soil types were used in Experiment 2. Three soil types were collected from the same sites selected in Experiment 1. In addition, to study the key mechanisms involved in AM fungal–bacterial interactions in high P conditions, we selected a black soil (Olsen inorganic P (Olsen-Pi): 48 mg^{-1} kg) collected from Jilin Province (DB, 43°54′E, 125°18′N; Table S1). The microcosm units were separated by a 30-μm mesh into root compartments (length × width × height: 5 × 10 × 15 cm) and hyphal compartments (5 × 10 × 15 cm; Fig. S1d). Similarly, we put the sterilized membranes with 0.45-μm pores in each hyphal compartment to collect the hyphae (Fig. S1d). The effect of plant species on the hyphosphere microbiome was negligible in Experiment 1, so we selected one species, maize (Zhengdan 958), as the host plant. We targeted specific AM fungal species to simplify the AM fungal–bacterial interaction network. Therefore, the AM fungal strain *Rhizophagus intraradices* EY108 (*R. intraradices*) was selected as an inoculant, which was purchased from the International Collection of (Vesicular) Arbuscular Mycorrhizal Fungi (West Virginia University,

Morgantown, WV, USA). *Rhizophagus intraradices*, formerly named *Glomus intraradices*, corresponded to *Glomus* sp. in Experiment 1, which belonged to high abundance taxa. At planting, part of the soil (600 g) was carefully added to the root compartment, and then 60 g AM fungal inoculum, propagated on maize roots consisting of spores, mycelium, fine root segments, and soil and zeolite, was placed on the top of soil. Three pregerminated seeds were sown, and the remaining 250 g soil was added to the root compartment. The control treatments received the same amount of sterilized inoculum with 10 ml filtered washings of this inoculum. The filter was used to remove AM fungal propagules but maintain similar starting bacterial communities (Methods S1).

The microcosm experiment contained the following treatments: four soil types, including acidic red soil, loessial soil, gray desert soil, and black soil, with or without AM fungal inocula. Each treatment had six replicates; thus, there were 48 microcosms in total. Further details of the experimental setup are given in the Supporting Information.

Harvest and sample preparation

In Experiment 1, all in-growth tubes in each location were excavated, and the crop plant roots were collected at maturity, that is, 90 d after being buried. The membranes in the in-growth tubes were removed and stored at −80°C for collecting the hyphae. Soil samples were removed from the tubes and mixed well: Part of the soil was immediately frozen at −80°C ahead of DNA extraction. The other part of the soil was stored at −20°C to determine the phosphatase activity, −4°C to determine soil moisture content and air-dried to determine hyphal length density (HLD) and soil chemical properties. In Experiment 2, the plants were harvested 70 d after planting. All membranes in the hyphal compartments were removed from soil and stored at −80°C for collecting the hyphae. The process for soil samples in hyphal compartments was maintained as in Experiment 1.

Determination of mycorrhizal colonization, HLD, soil phosphatase activity, and P contents

Mycorrhizal colonization of roots was measured using the trypan blue staining method, and M% was quantified (Trouvelot *et al.*, 1986). Extraradical hyphae were extracted from two portions of 5 g air-dried soil using the membrane filter technique (Staddon *et al.*, 1999). Hyphal length was assessed using the gridline intercept method at ×200 magnification and then converted to HLD (m g^{-1} DW soil). Determination of alkaline phosphatase (ALP) and acid phosphatase (ACP) in the soil was performed using *p*-nitrophenyl phosphate (Tabatabai & Bremner, 1969). The Olsen organic P (Olsen-Po) in the $NaHCO_3$ was determined using the potassium persulfate oxidation method (Schoenau & Huang, 1991).

DNA extraction, PCR, and sequencing

The hyphae accumulated on the surface of membranes (Fig. S1e) were manually collected using a stereoscope. Arbuscular mycorrhizal fungal hyphae can be selected based on their different morphology from other fungi, as they are colorless and transparent, and have no septum. The collected hyphae were washed five times in washing buffers (0.01 M phosphate buffer saline, pH = 7) to remove the adhered soil. In Experiment 1, 10 mg of fresh hyphae (collected from the membrane of each in-growth tube that allowed AM fungi to grow into) was used for the extraction of DNA of AM fungi and their associated hyphosphere bacteria. The bulk soil (soil from in-growth tubes in which AM fungi were excluded) bacterial DNA was also extracted from 0.5 g of the collected soil. In Experiment 2, 10 mg of fresh hyphae was collected from each hyphal compartment for the extraction of DNA of hyphosphere bacteria. The DNA of bacteria in the bulk soil was extracted from 0.5 g of soil from each hyphal compartment under the noninoculation treatments. DNA extraction was performed using the FastDNA SPIN Kit for Soil (MP Biomedicals, Santa Ana, CA, USA).

To validate that the most of hyphae belong to AM fungi, we measured gene copy number of both the AM fungi and all fungi in our collected hyphal samples, and calculated the ratio of gene copy number of AM fungi vs all fungi to indicate the abundance of AM fungi against all fungi (Methods S1). The results showed that the abundance was > 90%, and consistent with the results of positive control (pure AM fungal hyphal samples collected from AM fungal inoculum) (Fig. S2). Therefore, we believed that the vast majority of the hyphae we collected were AM fungal hyphae.

To identify the AM fungal taxa in Experiment 1, an *c.* 334 bp region of 18S rRNA gene was amplified with a two-step PCR (Yang *et al.*, 2018). To identify the bacterial taxa in both experiments, the V3–V4 regions of the bacterial 16S rRNA gene were amplified with primer pairs 338F and 806R (Sakurai *et al.*, 2008).

Three pools of PCR products were prepared for sequencing: The first pool contained 18S rRNA gene amplicons from Experiment 1, the second contained 16S rRNA gene amplicons from Experiment 1, and the third contained 16S rRNA gene amplicons from Experiment 2. These pools were sent for sequencing to the Allwegene Tech. (Beijing, China) used an Illumina Miseq PE300 (San Diego, CA, USA) pyrosequencing platform. The details of bioinformatic processing were summarized in the Supporting Information.

Statistical analysis

Alpha and beta diversity All analyses were conducted using the R software (v.4.1.2), unless otherwise stated. Rarefaction curves were drawn for each individual sample to ensure sufficient sequencing depth (Fig. S3). Arbuscular mycorrhizal fungal and bacterial beta-diversities were assessed by computing the Bray–Curtis matrices and then visualized using principal coordinate analyses (PCoAs). The significance of experimental sites on microbial community structures was tested with PERMANOVA using the VEGAN package (Dixon, 2003). The fundamental function of co-inertia analysis (CoIA) is to match two datasets and project their variables in the same space to visualize their co-variations. The CoIA was performed with the ADE4 package to display the relationships between AM fungal communities and

hyphosphere bacterial communities (Iffis *et al.*, 2016). A variance partitioning analysis was performed by the varpart function in VEGAN package, to explore the relative contribution of AM fungal community structure, crops (maize and cotton), and environmental factors (soil pH, soil organic matter, water content, P content, etc.) on the shifts in hyphosphere bacterial communities. Significance levels according to Monte Carlo permutation tests were carried out with 1000 permutations.

Identification of hyphosphere-specific enriched OTUs and experimental site-sensitive or insensitive OTUs For both experiments, we employed complementary approaches to determine which operational taxonomic units (OTUs) were responsible for the observed effects (Hartman *et al.*, 2018). To determine the selection effect by AM fungi, we tested for differential bacterial OTUs abundance between hyphosphere and bulk soil communities at each site using likelihood ratio tests (adjusted $P < 0.05$) in the EDGER package, respectively, and then visualized using Manhattan plots (Robinson *et al.*, 2010). We identified the overlap of OTUs enriched in the hyphosphere among three experimental sites as hyphosphere-specific enriched OTUs (*hs*OTUs).

Additionally, in Experiment 1, we tested for differential OTUs abundance among different experimental sites using likelihood ratio tests with the EDGER package, and indicator species analysis with the indicspecies package, respectively (De Caceres *et al.*, 2010). Operational taxonomic units whose abundances were determined to be differing between one or more of the experimental sites at an adjusted $P < 0.05$ were considered to be experimental site responsive. Finally, we delimited OTUs that were calculated by both methods as experimental site-sensitive or -insensitive OTUs (*ss*OTUs or non-*ss*OTUs). In Experiment 2, the soil type-sensitive OTUs and soil type-insensitive OTUs (also abbreviated *ss*OTUs and non-*ss*OTUs) were also calculated in the same method above.

Co-occurrence networks For all networks, Spearman correlation scores were calculated, and only robust (Spearman's $r > 0.8$) and statistically significant ($P < 0.01$) correlations were kept. These networks were visualized with the Fruchterman–Reingold layout with 10^3 permutations in IGRAPH. For the in-depth assessment of microbial communities, we performed Spearman rank correlations between all pairs of bacteria (in Experiments 1 and 2) and all pairs of AM fungal OTUs (only in Experiment 1), separately.

We also constructed a meta-network to visualize correlations between hyphosphere bacteria and AM fungi in Experiment 1. For this, the TMM ('trimmed means of M' method with the package EDGER) and normalized CPM (relative abundance counts per million) counts of bacteria and AM fungi were combined, and used to perform Spearman rank correlations between all pairs of hyphosphere bacterial and AM fungal OTUs. To explore community structure within this hyphosphere meta-network, we identified the substructures of nodes with a greater density of edges within groups as network modules. For this, we utilized the *greedy optimization of modularity* algorithm as implemented in IGRAPH (Clauset *et al.*, 2004).

Results

AM fungal–hyphosphere bacterial interactions promote Po mineralization in the field

The large degree of mycorrhizal colonization (11.43–26.67%) confirmed that plant roots were successfully colonized by AM fungi, and large HLD (5.31–9.86 m g^{-1} soil) in the AM fungi-permitted tubes confirmed that a large number of extraradical hyphae extended into the in-growth tubes (Fig. S4). Phosphorus contents and phosphatase activities in the in-growth tubes that excluded AM fungi were subtracted from those that permitted AM fungi to derive the effects of AM fungal–hyphosphere bacterial association on the soil Po utilization. Two types of in-growth tubes were buried in the field and were spatially paired, and this allowed subtraction to be calculated between these pairs. At each site, the Olsen-Pi and Olsen-Po were reduced when AM fungi were allowed to grow into the tubes (Wilcoxon rank sum test, $P < 0.05$; Fig. 1a,b). Correspondingly, both ALP and ACP activities were significantly enhanced in the tubes into which AM fungi were permitted (Fig. 1c,d). Furthermore, both ALP and ACP activities differed across the three sites based on Olsen-Pi, and ACP activities were significantly negatively correlated with soil pH (Fig. S5).

Hyphosphere microbiome diversity varied across experimental sites

In total, 230 OTUs of AM fungi were detected in hyphal samples across the three experimental sites, of which only 28 OTUs were shared among all sites, but these shared OTUs accounted for 19.0% of the average relative abundance. The most abundant AM fungal taxa were members of the *Paraglomus*, *Ambispora*, and *Glomus* (Fig. 2a). The Kruskal–Wallis tests performed on AM fungal genera revealed that experimental sites significantly affected the relative abundance of *Archaeospora* ($P < 0.05$; Fig. 2a). Principal coordinate analysis of AM fungal OTUs matrices, based on weighted Bray–Curtis distances, revealed a trend toward significance in the separation of AM fungal communities among the three sites ($P = 0.09$; Fig. 2b).

A total of 26 188 sequences were retrieved from the 16S rRNA gene dataset for the hyphal and bulk soil samples and were assigned to 9780 bacterial OTUs. The species richness and diversity of bacteria decreased sharply from the bulk soil to the hyphosphere (Wilcoxon rank sum test, $P < 0.001$; Fig. S6). At high taxonomic ranks, hyphosphere bacterial communities were differentiated from each other and from the bulk soil, with communities being dominated by Actinobacteria (average 33.3% relative abundance of hyphosphere bacterial communities), and Alphaproteobacteria (18.2%; Fig. 2c).

A PCoA revealed a clear separation of bacterial communities clustering between the hyphosphere and bulk soil along the first coordinate axis, indicating strong influence of AM fungi on bacterial communities (Fig. 2d). For hyphosphere bacterial communities, PCoA combined with PERMANOVA analysis showed that the structure of bacterial communities was significantly affected by experimental sites (R^2 = 41%, $P < 0.001$).

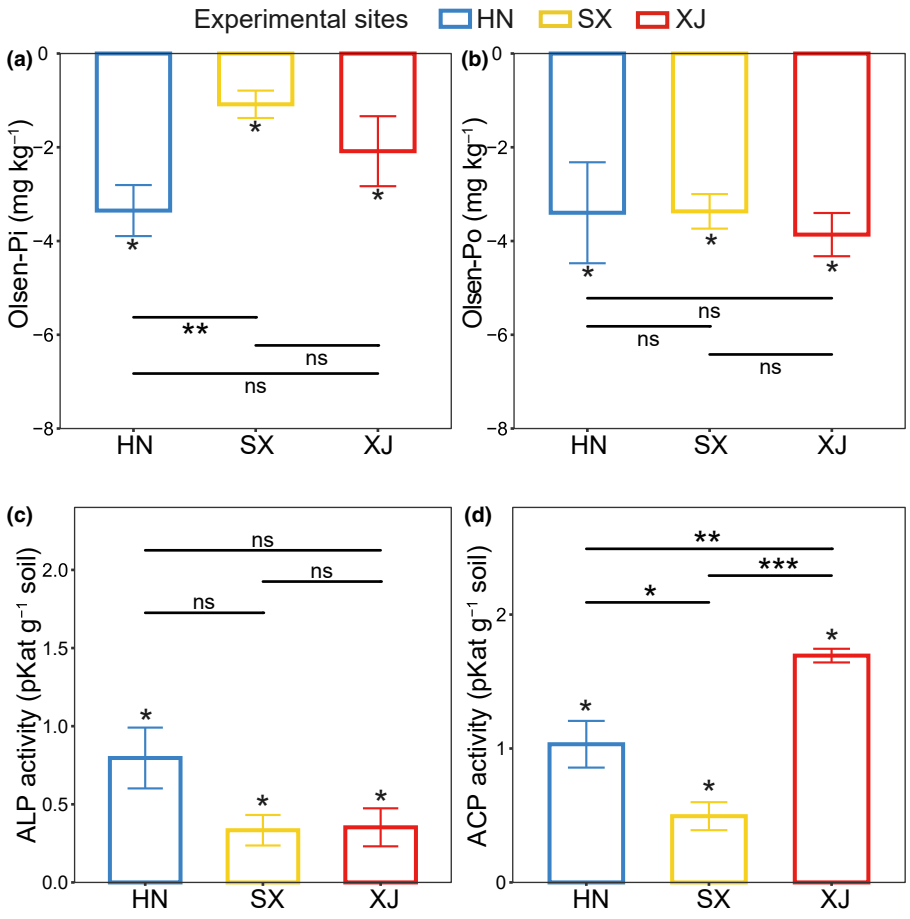

Fig. 1 Effects of arbuscular mycorrhizal (AM) fungal–bacterial association on organic P (Po) utilization. Difference of phosphorus (P) contents and phosphatase activities in the in-growth tubes buried in different sites with and without the presence of AM fungi. (a) Olsen-Pi, (b) Olsen-Po, (c) alkaline phosphatase (ALP) activity, and (d) acid phosphatase (ACP) activity in the in-growth tubes harvested at maturity. Values are means ($n = 8$) and bars represent SEs. A Student's *t*-test was performed to compare the significant difference. The asterisks near the lines indicate significant differences among three sites; the asterisks near the error bars indicate significant differences between the in-growth tubes with and without the presence of AM fungi. *, $P < 0.05$; **, $P < 0.01$; ***, $P < 0.001$; ns, no significance.

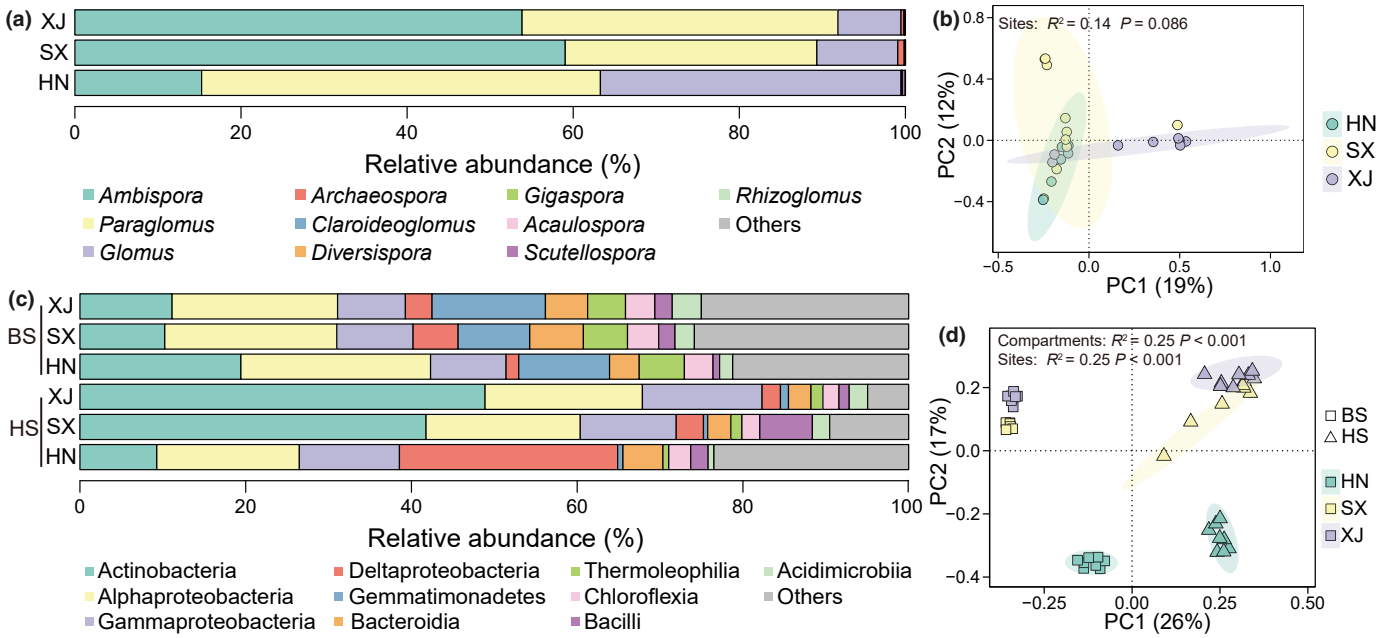

Fig. 2 Effects of experimental sites on hyphosphere bacterial communities. Histogram diagram showing the relative abundances of major genera of arbuscular mycorrhizal (AM) fungi contained in the hyphal samples (a), and major classes of bacteria in the hyphosphere and bulk soil (c) across three experimental sites. Principal coordinate analysis based on Bray–Curtis dissimilarity matrix of AM fungi (b) and bacteria (d). The contribution of explanatory variables on microbial community structures are listed. The significance of experimental factors on microbial community structures was tested with PERMANOVA. HS, hyphosphere; BS, bulk soil in the in-growth tubes which AM fungi were excluded from; XJ, Xinjiang; SX, Shaanxi; HN, Hunan.

Hyphosphere bacterial community in the HN site formed a distinct group along the second coordinate axis, indicating that experimental sites were also a large source of variation in the hyphosphere microbiome (Fig. 2d).

Identifying *ss*OTUs and non-*ss*OTUs

To further clarify microbial variation among experimental sites, we calculated *ss*OTUs and non-*ss*OTUs of AM fungi and bacteria based on whether it was more abundant at a specific site than any other site, and we summarized the analysis with a bipartite network (Fig. S7a,b). In the hyphosphere, a larger number of *ss*OTUs were shared between the SX and XJ sites, while a smaller number of *ss*OTUs were shared between the HN and SX or XJ sites (Fig. S7b). These patterns were similar to the effects in the β-diversity analyses, with the close clustering of the SX and XJ samples in the ordination.

As an approximation for 'effect size' of experimental sites on bacterial communities, we observed that 2684 bacterial *ss*OTUs in the bulk soil accounted for 83.8% of the total soil community OTUs. Similarly, we identified 910 *ss*OTUs for the hyphosphere bacteria, corresponding to an effect size of 42.6%. The smaller 'effect size' of experimental sites, that is, the larger amount of non-*ss*OTUs, indicated that the hyphosphere microbiome encompassed an unmissable constant core portion when examined across multiple hosts and environments. We only found one fungal *ss*OTUs, indicating that fungal locational variation was more quantitative than bacteria. These non-*ss*OTUs comprised a taxonomically broad set of bacteria and did not target specific microbial lineages (Fig. S7c).

AM fungal communities induced variation in hyphosphere bacterial communities

We noted that compositional differences in hyphosphere bacterial communities were evident across different sites due to a combination of environmental factors and AM fungal communities. Therefore, we used a CoIA approach to study the relationships between AM fungal and bacterial communities. The CoIA revealed a marked synergistic co-variation between AM fungal and hyphosphere bacterial communities (RV = 0.29, $P < 0.05$; Fig. 3a), with the first and second axes of the CoIA explaining 77.50% and 16.00% of the total projected inertia. Arrow lengths indicated the degree of concordance between AM fungal and hyphosphere bacterial communities for each sample, and the best agreements were observed in the shortest lengths. The arrow lengths did not show an obvious pattern of variation across three sites, indicating that experimental sites were not determinant of the concordance between AM fungal and hyphosphere bacterial communities (Fig. 3a). Further support for the robust association between AM fungal and hyphosphere bacterial community was provided by a variance partitioning analysis, which revealed that AM fungal communities explained a total contribution of 19% of the variability in hyphosphere bacterial communities, greater than environmental factors and plant species (Fig. 3b). The Mantel test also indicated the significant correlations between these two groups (Mantel statistic R: 0.32, $P < 0.001$).

Preferential associations between AM fungal and hyphosphere bacterial genera were also calculated (Fig. 3c,d). Those AM fungal genera pointing in the same direction as that of the hyphosphere bacterial genera are positively correlated, whereas those pointing in the opposite direction are negatively correlated. These relations were supported by the spearman correlations test across all experimental sites (Fig. 4a). For example, *Paraglomus* was significantly positively correlated with *Nocardioides* (Fig. 4a). Also calculated was the AM fungal–bacterial associations at each site, which were most complex at the HN site (Fig. 4b–d).

Identifying *hs*OTUs

We analyzed the enrichment of hyphosphere bacterial OTUs compared with the bulk soil and visualized them by Manhattan plots (Fig. 5a). At each site, likelihood ratio tests revealed a distinction of OTUs between the hyphosphere and bulk soil: At the HN site, 676 OTUs were significantly enriched in the hyphosphere accounting for 54.2% of the cumulative abundance of total OTUs; at the SX site, 420 OTUs were significantly enriched in the hyphosphere accounting for 53.2%; at the XJ site, 531 OTUs were enriched in the hyphosphere accounting for 58.0% (Fig. 5a).

To further explore the bacterial taxa closely related to AM fungi, we detected a notable overlap of OTUs enriched in the hyphosphere across the three experimental sites: only 82 *hs*OTUs (Fig. 5b). These 82 *hs*OTUs only accounted for 0.3% of all bacterial OTUs detected in the samples, but accounted for 30.2%, 21.1%, and 21.0% of the relative abundance for the HN, SX, and XJ sites, respectively. Furthermore, we noted that up to 60% of *hs*OTUs also belonged to non-*ss*OTUs, suggesting that their abundance was relatively stable (Fig. S8).

These *hs*OTUs comprised a taxonomically definite set of bacteria. At the class level, most *hs*OTUs belonged to Alphaproteobacteria, Actinobacteria, and Gammaproteobacteria. While at the order level, most *hs*OTUs belonged to Rhizobiales and Myxococcales (Fig. 5c). Furthermore, we found that many members in *hs*OTUs, especially those belonging to non-*ss*OTUs, were positively correlated with phosphatase activities (Fig. S8).

*hs*OTUs in the microbial co-occurrence network

Consistent with the α-diversity analyses, the bulk soil bacterial network comprised a greater number of significantly co-occurring nodes and greater connectivity than that of hyphosphere networks (Fig. S9). Meanwhile, the *ss*OTUs were also mapped into each network, and they agglomerated in line with different experimental sites (Fig. S9). The *ss*OTUs in the bulk soil network were up to 94%, but it dropped to 55% in the hyphosphere, suggesting the strong influence of AM fungi on the hyphosphere microbiome.

We focused mainly on the distribution patterns of *ss*OTUs and *hs*OTUs in meta co-occurrence patterns of AM fungal and hyphosphere bacterial communities (Fig. 6a). The abundance patterns of interkingdom microbial associations also responded to different experimental sites. Modules are substructures of nodes with a higher density of edges within groups than between

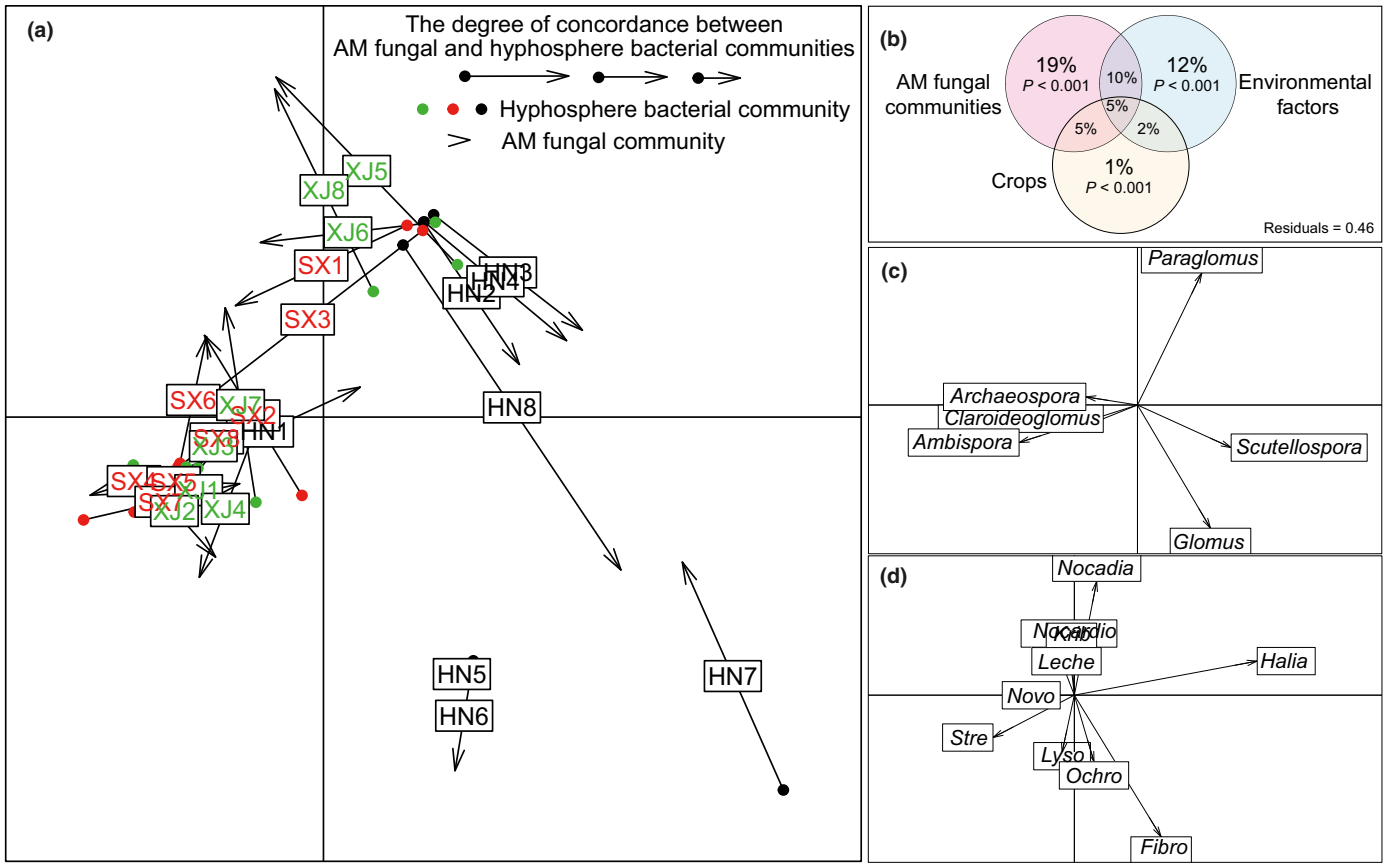

Fig. 3 Co-inertia analysis (CoIA) showing the relationship between arbuscular mycorrhizal (AM) fungal and hyphosphere bacterial communities (RV = 0.29, $P = 0.02$). (a) Projection of both AM fungal genera and hyphosphere bacterial genera onto the co-inertia plane. The base of each arrow (closed circles) represents AM fungal community, while the tip represents bacterial community. The letters in the squares and their colors indicate different experimental sites, and the numbers after the letters represent different repetitions. (b) Variance partitioning of hyphosphere bacterial communities by AM fungal communities, environmental factors and crops. Significance levels according to Monte Carlo permutation tests were carried out with 1000 permutations. (c) Projection of AM fungal genera onto co-inertia plane. (d) Projection of hyphosphere bacterial genera onto co-inertia plane. Abbreviations shown in (d) indicate: *Fibro*, *Fibrobacteraceae*; *Halia*, *Haliangium*; *Krib*, *Kribbella*; *Leche*, *Lechevalieria*; *Lyso*, *Lysobacter*; *Nocardia*, *Nocardia*; *Nocardio*, *Nocardioides*; *Ochro*, *Ochrobactrum*; *Stre*, *Streptomyces*.

them, which reflected strongly correlated OTUs in the co-occurrence network. We noted in the hyphosphere meta co-occurrence network that two modules (modules 2 and 3) contained relatively high proportions of *ss*OTUs (Fig. 6a,b). The type of sensitivity of these module members to the specific experimental site and their distribution in the network partially reflected the drivers of community dissimilarity in the PCoA ordinations. In detail, the effect of the HN site in the hyphosphere communities was apparent with a discrete module (module 3) in the hyphosphere network, containing *ss*OTUs specific to the HN site. Module 3 was separated from module 2, which primarily contained *ss*OTUs specific to the SX and XJ sites (Fig. 6a,b).

The majority of *hs*OTUs, including most members belonging to non-*ss*OTUs (gray pentagram), were concentrated in module 4 (Fig. 6a,b), which contained a relatively small proportion of *ss*OTUs (Fig. 6b). These characteristics indicated that module 4, as the experimental sites nonsensitive and hyphosphere-specific enriched guild, might have a more intense association with AM fungi. Furthermore, we measured the copy numbers of general bacteria to reflect the absolute abundance of hyphosphere bacteria across the three sites. The results showed that there was no significant difference in the hyphosphere bacterial abundance among different sites (Fig. S10). Based on this, the trend of relative and absolute abundance of modules could be consistent. A strong and significant positive association between the relative abundance of module 4 and ALP or ACP activity was found, hinting that module 4 played a considerable part in the mineralization of Po (Fig. 6c).

The microcosm experiment testing the core *hs*OTUs taxa

After the characterization of the hyphosphere bacterial communities *in situ* in the field, we sought to control perturbation of environmental parameters, and targeted the specific AM fungal species, to obtain further evidence of the stability of *hs*OTUs taxonomic composition, and their links to the Po mobilization. Therefore, we performed a compartmented microcosm experiment by inoculating with *R. intraradices* and using typical soil types corresponding to Experiment 1. Similar scenarios of Po mobilization appeared: Compared with the noninoculation treatment, both ACP and ALP activities were significantly increased, and the Po content was

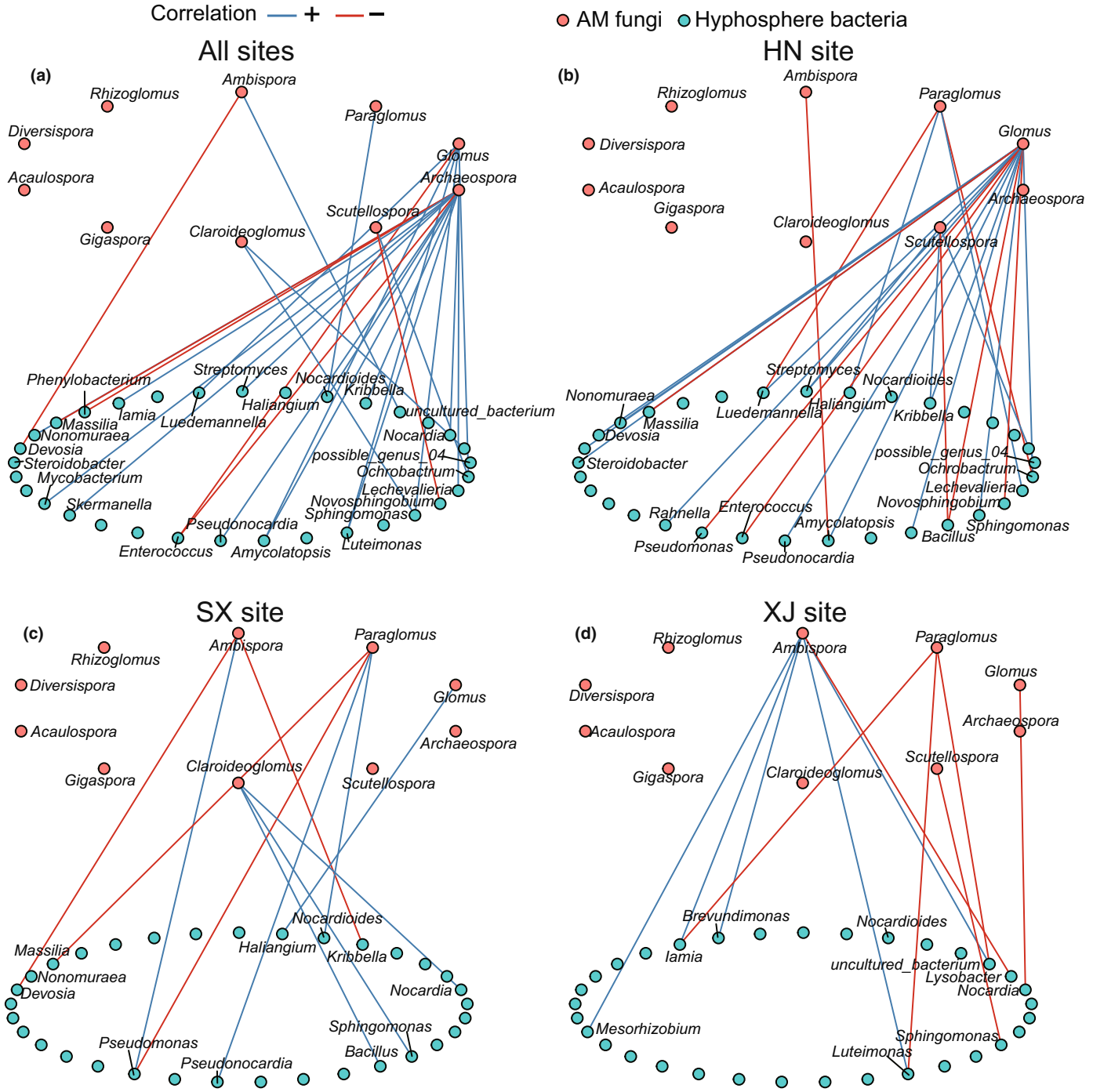

Fig. 4 Network analysis showing Spearman correlations between arbuscular mycorrhizal (AM) fungal and hyphosphere bacterial genera across all sites (a) or at each site (b–d). Red circles indicate AM fungi, blue circles indicate hyphosphere bacteria. The blue lines indicate significantly positive correlations, while the red lines indicate significantly negative correlations ($P < 0.05$). HN, Hunan; SX, Shaanxi; XJ, Xinjiang.

significantly decreased in hyphal compartments in the inoculation treatment (Figs S11, S12). The most abundant taxa in the hyphosphere were members of the Betaproteobacteriales, Pseudomonadales, and Rhizobiales (Fig. S13a). Analysis of diversity revealed that hyphosphere showed a distinct bacterial community compared with the bulk soil (Figs 7a, S13b).

Next, we sought to assess whether the observed bacterial taxa closely related to AM fungi in the field could be extended to this microcosm experiment. We also identified *ss*OTUs and *hs*OTUs as described above. We observed that 68 *hs*OTUs only accounted for 0.5% of all bacterial OTUs detected in the samples, but the aggregated relative abundance of these *hs*OTUs ranged from 16% to 29% in their respective communities (Fig. S13c). At a high taxonomic rank, *hs*OTUs exhibited an extremely similar taxonomic composition between the field and microcosm, albeit with differing counts (Fig. 7b). For example, at the class level, we

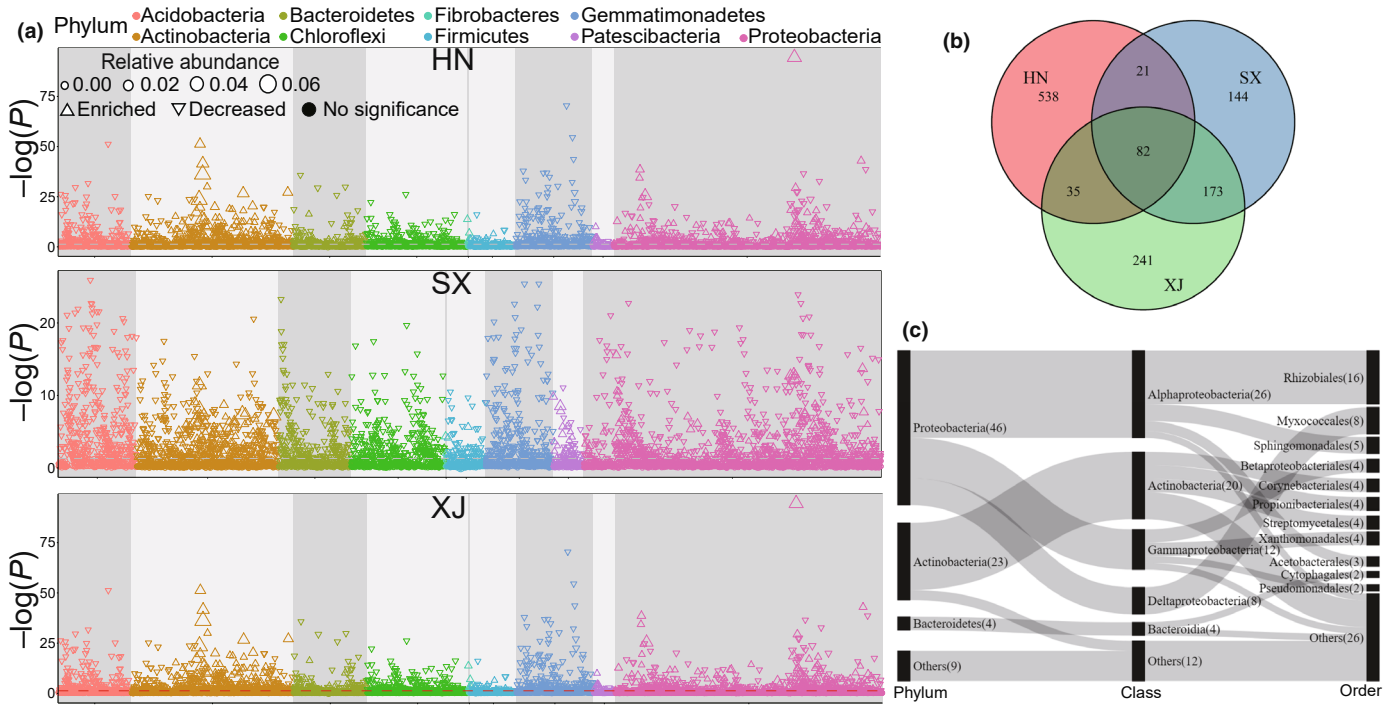

Fig. 5 Hyphosphere harbor specific sets of bacteria. (a) Manhattan plots showing bacterial operational taxonomic units (OTUs) enriched in the hyphosphere compared with bulk soil. Operational taxonomic units enriched or diminished in the hyphosphere are represented by up-facing triangles or down-facing triangles, respectively (likelihood ratio tests: false discovery rate corrected value of $P < 0.05$). (b) Venn plot showing the number of OTUs enriched in the hyphosphere at each site. (c) Qualitative taxonomic composition of 82 *hs*OTUs (shown in b) is reported as the count of OTUs per phylum, class and order. HN, Hunan; SX, Shaanxi; XJ, Xinjiang.

observed that *hs*OTUs were dominated by Alphaproteobacteria, Actinobacteria, and Gammaproteobacteria in both experiments (Fig. 7b). The major difference of *hs*OTUs taxa between two experiments was given by the members with smaller counts.

Finally, we mapped *ss*OTUs and *hs*OTUs in the hyphosphere bacterial co-occurrence network. These *ss*OTUs agglomerated according to soil types, with most *hs*OTUs belonging to non-*ss*OTUs (gray pentagram) concentrated in independent modules (module 15 and module 30), which were clearly separated from *ss*OTUs (Fig. 7c,d). Both module 30 in Experiment 2 and module 4 in Experiment 1 were dominated by Actinobacteria, Alphaproteobacteria, and Gammaproteobacteria (Fig. S14). We also observed a strong and significant positive association between the relative abundance of module 30 and ALP or ACP activity (Fig. 7e). Taken together, these results further indicate that major members of *hs*OTUs were conserved at a high taxonomic rank and contributed to the soil Po mineralization.

Discussion

Extensive fungal diversity exists in a single plant root (Vandenkoornhuyse *et al.*, 2002; Powell & Rillig, 2018), while the extraradical hyphae of co-colonizing fungi are colonized by complex bacterial communities (de Boer *et al.*, 2005; Zhou *et al.*, 2020). Although such fungal–bacterial interactions are crucial to many biogeochemical processes, for example, soil C, N, and P turnover and cycling (Hodge & Fitter, 2010; Cheng *et al.*, 2012; Zhang *et al.*, 2018b; Rozmos *et al.*, 2022), how the cross-kingdom consortia affect important ecological functioning and whether there is a universal group of functional bacteria is less well-understood. In the present study, we performed field sampling across three climate zones, and further validated our findings with a controlled microcosm experiment. Our results showed that although AM fungi harbored distinct bacterial communities in each soil type, some bacterial members were consistently enriched in the hyphosphere, and gathered into an independent module in the fungal–bacterial interaction network. Moreover, their abundance was significantly related to phosphatase activity, which suggested that the AM fungal–bacterial consortia shared a functionally relevant core microbiome across broad environments.

Which factors drive the formation of hyphosphere microbiome?

Understanding the drivers of hyphosphere bacterial assemblages under field conditions is a crucial step toward developing management strategies to obtain a bacterial community structure favoring AM fungal functioning. To date, scattered studies have shown that hyphosphere microbiomes may vary with biotic and abiotic factors, such as AM fungal species and soil P forms (Wang *et al.*, 2016; Zhou *et al.*, 2020; Emmett *et al.*, 2021). But these studies are usually conducted in controlled conditions such as glasshouses where abiotic conditions were manipulated, and mainly focused on the hyphae-associated bacteria of specific AM fungal species. There is still a substantial gap between studies performed in laboratory conditions and the '*in situ*' reality

New Phytologist

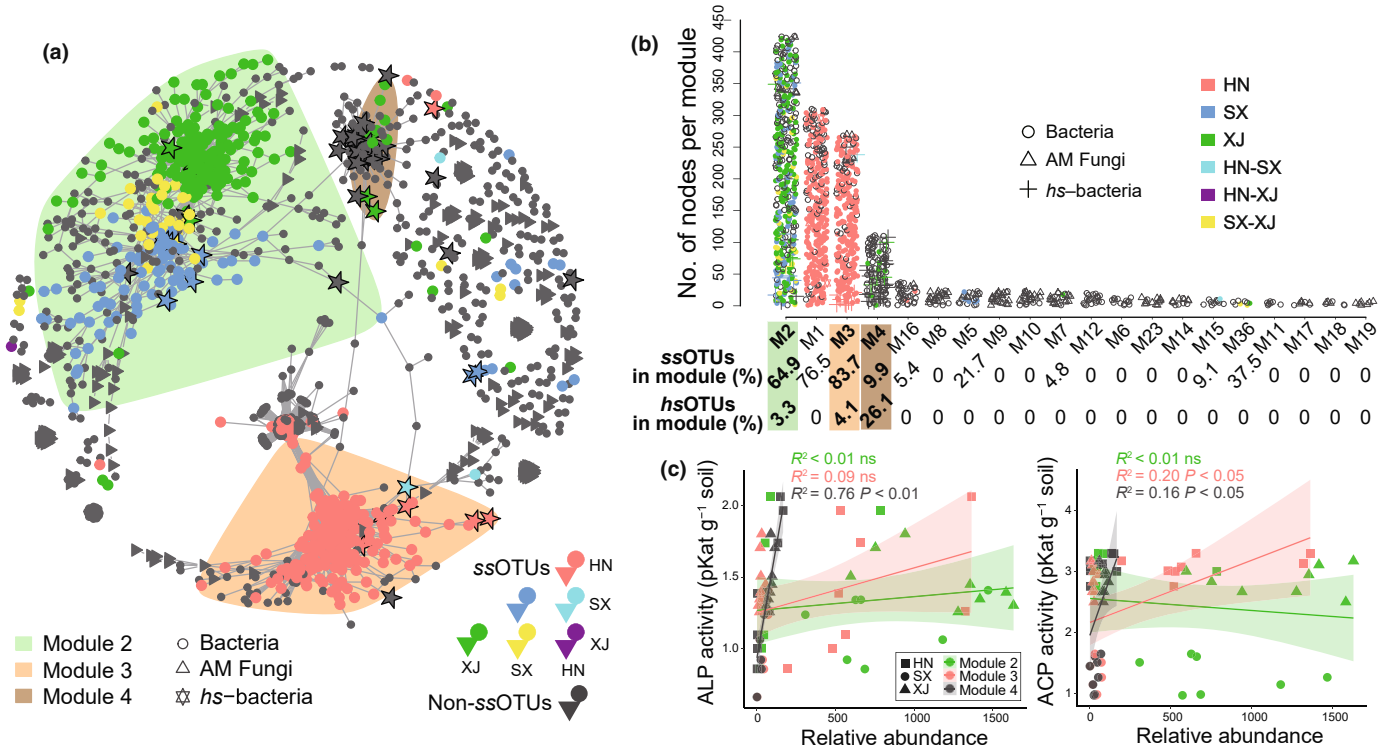

Fig. 6 Co-occurrence patterns of *ss*OTUs, non-*ss*OTUs, and *hs*OTUs. (a) Co-occurrence networks visualizing significant Spearman correlations ($r > 0.8$, $P < 0.01$; indicated with gray lines) between hyphosphere bacterial operational taxonomic units (OTUs) and arbuscular mycorrhizal (AM) fungal OTUs. Circles, triangles, and stars represent bacteria, AM fungi and *hs*OTUs, respectively. Operational taxonomic units are colored by their association with the different experimental sites. Shaded areas represent the network modules containing *ss*OTUs, non-*ss*OTUs, and *hs*OTUs. (b) Plots showing the amount of OTUs in the top 20 most populated modules in the hyphosphere meta co-occurrence networks (shown in a). Circles, triangles, and crosses represent bacteria, AM fungi and *hs*OTUs, respectively. Colors indicate the association of OTUs to the different experimental sites. (c) Spearman correlations between ALP or ACP activity and the relative abundance (as counts per million, CPM) of the modules.

that impedes our ability to extrapolate generic principles of fungal-bacterial interactions at the community scale (Deveau *et al.*, 2018).

The present study was set up in three field sites, which covered humid, semiarid, and arid climate zones and contrasting soil types, to explore the effect of environmental variation, plant species, and AM fungal community identity on hyphosphere microbiome *in situ*. First, our results found that different plants (i.e. maize and cotton) had little influence on the hyphosphere bacterial community (Fig. 3d), which was consistent with previous studies (Zhang *et al.*, 2018b). Lipids are transferred from the plant host to AM fungi as a major carbon source (Jiang *et al.*, 2017; Luginbuehl *et al.*, 2017). Although AM fungi receive all of the required C from plants, there is no evidence that the forms of C varied with plant species. It can be speculated that the influence of plant species on the hyphosphere microbiome is subtle, far less than that of AM fungal species itself. Second, although both AM fungal and hyphosphere bacterial communities were affected by experimental sites, we identified a significant correlation between AM fungal community and hyphosphere bacterial community composition (Figs 2, 3). This implied that AM fungal species with different morphological, physiological, and genetic characteristics coexisted in the community and co-orchestrated the distinct hyphosphere microbiome through variation in the composition of exudates to cope with the environment factors (Zhou *et al.*, 2020; L. Zhang *et al.*, 2022).

Does the hyphosphere of AM fungi harbor a core microbiome?

A core microbiome is defined as a suite of potentially crucial microbes shared within a host microhabitat (Hernandez-Agreda *et al.*, 2017; Shade & Stopnisek, 2019). This concept was first applied to understand the bacterial communities that are associated with humans, followed by plants including roots and leaves (Shade & Handelsman, 2012; Vandenkoornhuyse *et al.*, 2015). The hyphosphere microbiome encompasses bacteria inhabiting the hyphal surface, and it represents the close association between AM fungi and bacteria. The hyphosphere bacterial communities are largely different from those in the bulk soil (Scheublin *et al.*, 2010; Nuccio *et al.*, 2013; Zhang *et al.*, 2018b). However, research has yet to determine the stability of the vast majority of hyphosphere bacterial associations of AM fungi, and the identity and functional contribution of the core microbiome in the hyphosphere is missing.

A variety of study-specific approaches have been used to define the core microbiome in the recent literature: abundance-defined cores informed by ranked abundance curves; detection-defined cores

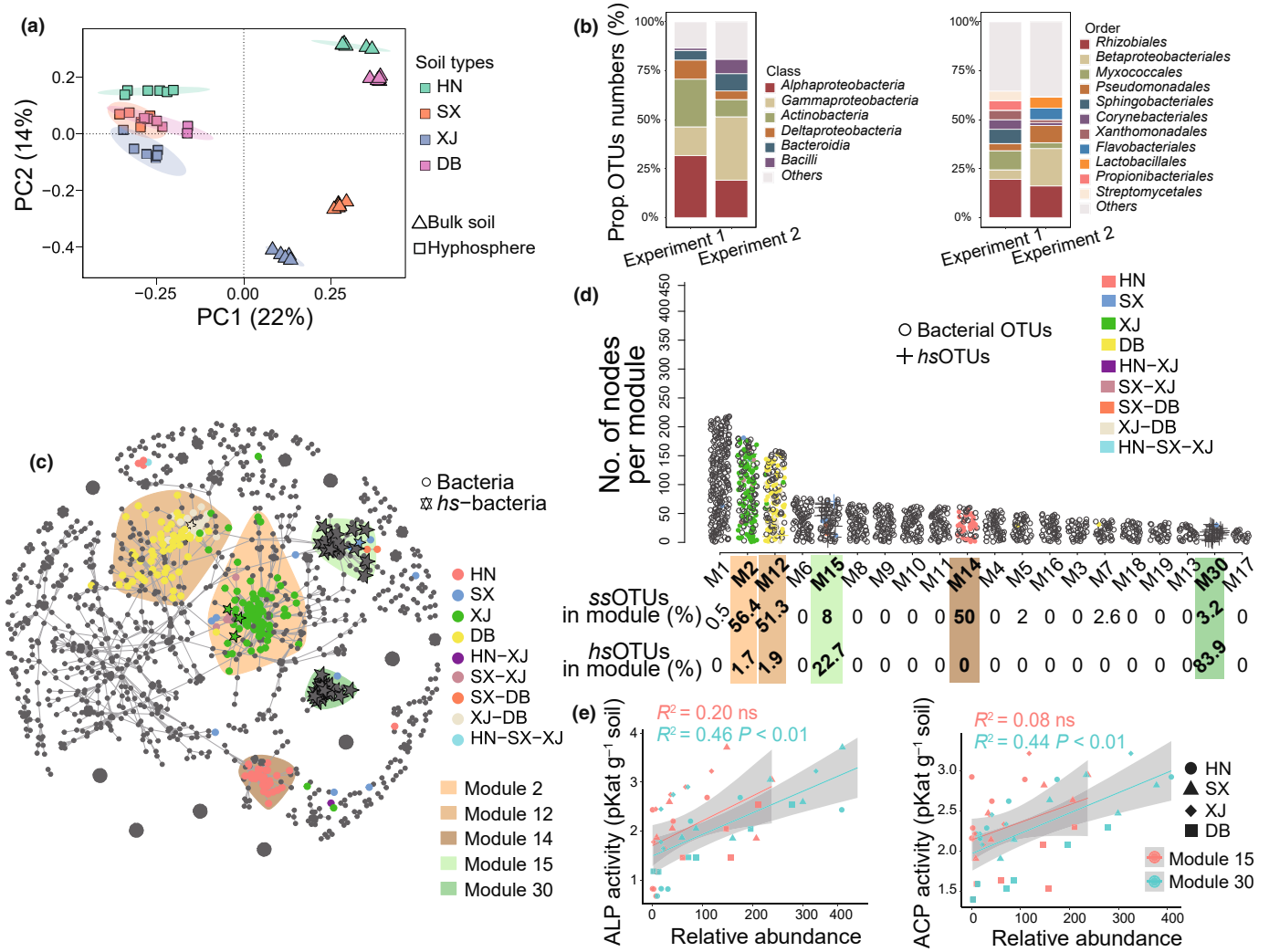

Fig. 7 Effects of soil type on hyphosphere bacterial communities. (a) Principal coordinate analysis (PCoA) based on the Bray–Curtis dissimilarity matrix of hyphosphere bacteria across four soil types. (b) Qualitative taxonomic composition of *hs*OTUs is reported as proportional operational taxonomic units (OTUs) numbers per class or order. (c) Co-occurrence networks visualizing significant Spearman correlations ($r > 0.8$, $P < 0.01$; indicated with gray lines) between hyphosphere bacterial OTUs. (d) Plots showing the amount of OTUs in the top 20 most populated modules in the hyphosphere bacterial networks. (e) Spearman correlations between ALP or ACP activity and the relative abundance (as counts per million, CPM) of the module 15 and 30. HN, SX, XJ, and DB indicate acidic red soil, loessial soil, gray desert soil, and black soil, respectively.

informed by Venn diagram; comparison-cores by enrichment in particular conditions; network-cores by microbial network analysis (Shade & Handelsman, 2012; Banerjee *et al.*, 2018; Shade & Stopnisek, 2019). Here, although the hyphosphere microbiome encompassed largely variable portions when examined across different climate zones, we identified and emphasized *hs*OTUs in the field experiment, which were enriched in the hyphosphere and shared by AM fungal consortia across multiple environmental factors and plant species. A striking-specific distribution pattern of these *hs*OTUs in the meta-co-occurrence network was observed: They gathered into an independent and experimental site nonsensitive module. Furthermore, in the microcosm experiment within which abiotic factors and AM fungi were manipulated, we can still detect similar results as the field experiment regarding the stable taxonomic composition of *hs*OTUs and their distinct distribution in the network. It is possible, therefore, that these *hs*OTUs may collectively constitute a core hyphosphere microbiome shared among AM fungal consortia. The core definition in this study incorporated aspects of detection, abundance, and the network analysis and can provide ecological insights into prioritize members that are selected by the AM fungi or adapted to the specific environment.

At a high taxonomic rank (class or order), the core hyphosphere microbiome exhibited a similar taxonomic composition between field and microcosm experiments (Fig. 6b). This implies that, similar to rhizosphere microbiomes, broad selection of AM fungi for particular phylogenetic bacteria is consistent across the changed environment. The core hyphosphere microbiome comprised of both well-known AM fungi-associated taxa and poorly characterized and as yet uncultured taxa, and mainly involved Rhizobiales, Betaproteobacteriales, Myxococcales, and Pseudomonadales (Figs 5c, 6b). Similarly, Emmett *et al.* (2021) found repeated enrichment for some bacterial members in the

hyphosphere across experiments and divergent soils under glasshouse conditions. Despite being in a completely different tested environments, most of these members also were observed in core hyphosphere microbiome in our study including Myxococcales, Betaproteobacteriales, Fibrobacterales, Cytophagales, and Chloroflexales, implying that these core taxa may be globally important hyphosphere bacteria. We cross-referenced the hyphosphere core taxa with those known root-associated cores of maize and cotton observed in previous studies (Table S2; Walters *et al.*, 2018; K. Zhang *et al.*, 2022). Several core taxa were shared, including Betaproteobacteriales, Pseudomonadales, and Rhizobiales. This overlap provided clues about 'generalist' members which may function in both the hyphosphere and rhizosphere.

It was hypothesized that the core microbiome composition would tend to be simpler as the hierarchical ecological level increases, and changed occurring through temporal and spatial variation at the given level (Vandenkoornhuyse *et al.*, 2015). In future studies, the hyphosphere core microbiome needs to be verified for consistency by more experiments across time and space, and we predict that the hyphosphere core microbiome could be considerably more restricted than the list provided in the present study.

What is the function of the hyphosphere core microbiome?

Interactions between soil fungi and bacteria are crucial to the functioning of ecosystems: They are major players in driving soil nutrient biogeochemical cycles, and contribute to both the health and the diseases of plants (Deveau *et al.*, 2018). Given the complexity of AM fungal–bacterial interactions and the dependence of those interactions on environmental conditions, the core microbiome provides a good point of entry to link fungal–bacterial co-occurrence patterns to soil ecosystem functions. This study, corroborating prior studies, has revealed that AM fungal–bacterial interactions strengthened phosphatase activity and stimulated Po mineralization (Zhang *et al.*, 2018b, 2020). Considering the inability of AM fungi to release phosphatases from their hyphae, the utilization of Po by AM fungi apparently relies on the recruitment of hyphosphere bacteria (Tisserant *et al.*, 2013; Zhang *et al.*, 2016). Therefore, we speculate that the functions of the hyphosphere core microbiome may be potentially important for the AM fungal P nutrient acquisition process.

Co-occurrence networks are an especially powerful tool to assess the complexity of potential AM fungal–bacterial interactions (Faust & Raes, 2012). Network patterns of the core microbiome provide community-wide status of the specialization and stability of AM fungal–hyphosphere bacterial interactions in the face of perturbations. In the AM fungal–bacterial interaction networks under *in situ* and glasshouse conditions, we observed that the members of hyphosphere core microbiome mainly grouped in the distinct guild, whose abundance was strongly and significantly positively associated with phosphatase activity (Figs 6, 7). Furthermore, a sizable subset in core microbiome members, including Rhizobiales, Sphingomonomonas, and Xanthomonadales, were positively associated with the phosphatase activity, implying that these members may promote the utilization of Po. This result supported our speculation on function of the core microbiome on Po mobilization, to a certain extent. However, inference of ecological function from OTU data must be interpreted cautiously. Hypotheses about functions of hyphosphere core microbiome need to be tested using (meta-) genome, (meta-) transcriptome sequencing, or synthetic communities with isolated strains to experimentally test how core microbiome affect AM fungi and even plant performance (Langille *et al.*, 2013; Bai *et al.*, 2015).

Conclusions

Taken together, we detected a core set of hyphosphere microbiome shared among AM fungal consortia and identified members of the core microbiome dominated by Alphaproteobacteria, Actinobacteria, and Gammaproteobacteria. This conserved core hyphosphere microbiome may potentially provide critical functions to the AM fungi by promoting Po utilization. Deploying core microbiomes are promising targets for optimizing beneficial bacterial functioning at the hyphosphere scale, thereby increasing plant nutrient uptake (Toju *et al.*, 2018). Our results have deepened our understanding of AM fungal–hyphosphere bacterial interactions at the community level and have important implications for comprehensive understanding the implication of fungal–bacterial interactions for biogeochemical processes.

Acknowledgements

We are thankful to Prof. Yang Bai from the Institute of Genetics and Developmental Biology, Chinese Academy of Sciences for his valuable technique support in bacterial isolation and identification. This study was financially supported by the National Natural Science Foundation of China (32272807, U1703232) and National Key R&D Program of China (2017YFD0200200). The contribution of TSG through The James Hutton Institute was supported by funds from the Rural and Environment Science and Analytical Services Division of the Scottish Government.

Competing interests

None declared.

Author contributions

GF and LW designed the study. LW, GF and LZ conducted sampling from the fields. LW performed the experiment and the data analyses. LW wrote the first version of the manuscript. GF, LZ and TSG provided valuable insight and ideas during numerous sessions of discussion. All authors provided critical comments on the manuscript and gave final approval for publication. LW and LZ contributed equally to this work.

ORCID

Gu Feng https://orcid.org/0000-0002-1052-5009
Timothy S. George https://orcid.org/0000-0003-3231-2159

Letian Wang https://orcid.org/0000-0002-7191-1376
Lin Zhang https://orcid.org/0000-0002-1663-5620

Data availability

Raw data used in this study are available in the NCBI Sequence Read Archive (SRA), accession no. PRJNA850088.

References

Agnolucci M, Battini F, Cristani C, Giovannetti M. 2015. Diverse bacterial communities are recruited on spores of different arbuscular mycorrhizal fungal isolates. *Biology and Fertility of Soils* **51**: 379–389.

Bai Y, Mueller DB, Srinivas G, Garrido-Oter R, Potthoff E, Rott M, Dombrowski N, Muench PC, Spaepen S, Remus-Emsermann M *et al.* 2015. Functional overlap of the *Arabidopsis* leaf and root microbiota. *Nature* **528**: 364–369.

Banerjee S, Schlaeppi K, van der Heijden MGA. 2018. Keystone taxa as drivers of microbiome structure and functioning. *Nature Reviews Microbiology* **16**: 567–576.

de Boer W, Folman LB, Summerbell RC, Boddy L. 2005. Living in a fungal world: impact of fungi on soil bacterial niche development. *FEMS Microbiology Reviews* **29**: 795–811.

Cheng L, Booker FL, Tu C, Burkey KO, Zhou LS, Shew HD, Rufty TW, Hu SJ. 2012. Arbuscular mycorrhizal fungi increase organic carbon decomposition under elevated CO_2. *Science* **337**: 1084–1087.

Clauset A, Newman MEJ, Moore C. 2004. Finding community structure in very large networks. *Physical Review E* **70**, 066111.

De Caceres M, Legendre P, Moretti M. 2010. Improving indicator species analysis by combining groups of sites. *Oikos* **119**: 1674–1684.

Deveau A, Bonito G, Uehling J, Paoletti M, Becker M, Bindschedler S, Hacquard S, Herve V, Labbe J, Lastovetsky OA *et al.* 2018. Bacterial–fungal interactions: ecology, mechanisms and challenges. *FEMS Microbiology Reviews* **42**: 335–352.

Dixon P. 2003. VEGAN, a package of R functions for community ecology. *Journal of Vegetation Science* **14**: 927–930.

Duplessis S, Cuomo CA, Lin YC, Aerts A, Tisserant E, Veneault-Fourrey C, Joly DL, Hacquard S, Amselem J, Cantarel BL *et al.* 2011. Obligate biotrophy features unraveled by the genomic analysis of rust fungi. *Proceedings of the National Academy of Sciences, USA* **108**: 9166–9171.

Duran P, Thiergart T, Garrido-Oter R, Agler M, Kemen E, Schulze-Lefert P, Hacquard S. 2018. Microbial interkingdom interactions in roots promote *Arabidopsis* survival. *Cell* **175**: 973–983.

Emmett BD, Levesque-Tremblay V, Harrison MJ. 2021. Conserved and reproducible bacterial communities associate with extraradical hyphae of arbuscular mycorrhizal fungi. *ISME Journal* **15**: 2276–2288.

Engelmoer DJP, Kiers ET. 2015. Host diversity affects the abundance of the extraradical arbuscular mycorrhizal network. *New Phytologist* **205**: 1485–1491.

Faust K, Raes J. 2012. Microbial interactions: from networks to models. *Nature Reviews Microbiology* **10**: 538–550.

Genre A, Lanfranco L, Perotto S, Bonfante P. 2020. Unique and common traits in mycorrhizal symbioses. *Nature Reviews Microbiology* **18**: 649–660.

Hartman K, van der Heijden MGA, Wittwer RA, Banerjee S, Walser J-C, Schlaeppi K. 2018. Cropping practices manipulate abundance patterns of root and soil microbiome members paving the way to smart farming. *Microbiome* **6**: 14.

Hernandez-Agreda A, Gates RD, Ainsworth TD. 2017. Defining the core microbiome in corals' microbial soup. *Trends in Microbiology* **25**: 125–140.

Hodge A, Fitter AH. 2010. Substantial nitrogen acquisition by arbuscular mycorrhizal fungi from organic material has implications for N cycling. *Proceedings of the National Academy of Sciences, USA* **107**: 13754–13759.

Iffis B, St-Arnaud M, Hijri M. 2016. Petroleum hydrocarbon contamination, plant identity and arbuscular mycorrhizal fungal (AMF) community determine assemblages of the AMF spore-associated microbes. *Environmental Microbiology* **18**: 2689–2704.

Jiang YN, Wang WX, Xie QJ, Liu N, Liu LX, Wang DP, Zhang XW, Yang C, Chen XY, Tang DZ *et al.* 2017. Plants transfer lipids to sustain colonization by mutualistic mycorrhizal and parasitic fungi. *Science* **356**: 1172–1175.

Johnson JB, Omland KS. 2004. Model selection in ecology and evolution. *Trends in Ecology and Evolution* **19**: 101–108.

Kiers ET, Duhamel M, Beesetty Y, Mensah JA, Franken O, Verbruggen E, Fellbaum CR, Kowalchuk GA, Hart MM, Bago A *et al.* 2011. Reciprocal rewards stabilize cooperation in the mycorrhizal symbiosis. *Science* **333**: 880–882.

Knegt B, Jansa J, Franken O, Engelmoer DJP, Werner GDA, Buecking H, Kiers ET. 2016. Host plant quality mediates competition between arbuscular mycorrhizal fungi. *Fungal Ecology* **20**: 233–240.

Langille MGI, Zaneveld J, Caporaso JG, McDonald D, Knights D, Reyes JA, Clemente JC, Burkepile DE, Thurber RLV, Knight R *et al.* 2013. Predictive functional profiling of microbial communities using 16S rRNA marker gene sequences. *Nature Biotechnology* **31**: 814–821.

Luginbuehl LH, Menard GN, Kurup S, Van Erp H, Radhakrishnan GV, Breakspear A, Oldroyd GED, Eastmond PJ. 2017. Fatty acids in arbuscular mycorrhizal fungi are synthesized by the host plant. *Science* **356**: 1175–1178.

de Menezes AB, Richardson AE, Thrall PH. 2017. Linking fungal-bacterial co-occurrences to soil ecosystem function. *Current Opinion in Microbiology* **37**: 135–141.

Mommer L, Cotton TEA, Raaijmakers JM, Termorshuizen AJ, van Ruijven J, Hendriks M, van Rijssel SQ, van de Mortel JE, van der Paauw JW, Schijlen EGWM *et al.* 2018. Lost in diversity: the interactions between soil-borne fungi, biodiversity and plant productivity. *New Phytologist* **218**: 542–553.

Neu AT, Allen EE, Roy K. 2021. Defining and quantifying the core microbiome: challenges and prospects. *Proceedings of the National Academy of Sciences, USA* **118**: e2104429118.

Nuccio EE, Hodge A, Pett-Ridge J, Herman DJ, Weber PK, Firestone MK. 2013. An arbuscular mycorrhizal fungus significantly modifies the soil bacterial community and nitrogen cycling during litter decomposition. *Environmental Microbiology* **15**: 1870–1881.

Powell JR, Rillig MC. 2018. Biodiversity of arbuscular mycorrhizal fungi and ecosystem function. *New Phytologist* **220**: 1059–1075.

Robinson MD, McCarthy DJ, Smyth GK. 2010. edgeR: a Bioconductor package for differential expression analysis of digital gene expression data. *Bioinformatics* **26**: 139–140.

Rozmos M, Bukovska P, Hrselova H, Kotianova M, Dudas M, Gancarcikova K, Jansa J. 2022. Organic nitrogen utilisation by an arbuscular mycorrhizal fungus is mediated by specific soil bacteria and a protist. *ISME Journal* **16**: 676–685.

Sakurai M, Wasaki J, Tomizawa Y, Shinano T, Osaki M. 2008. Analysis of bacterial communities on alkaline phosphatase genes in soil supplied with organic matter. *Soil Science and Plant Nutrition* **54**: 62–71.

Salvioli A, Ghignone S, Novero M, Navazio L, Venice F, Bagnaresi P, Bonfante P. 2016. Symbiosis with an endobacterium increases the fitness of a mycorrhizal fungus, raising its bioenergetic potential. *ISME Journal* **10**: 130–144.

Scheublin TR, Sanders IR, Keel C, van der Meer JR. 2010. Characterisation of microbial communities colonising the hyphal surfaces of arbuscular mycorrhizal fungi. *ISME Journal* **4**: 752–763.

Schoenau JJ, Huang WZ. 1991. Anion-exchange membrane, water, and sodium-bicarbonate extractions as soil tests for phosphorus. *Communications in Soil Science and Plant Analysis* **22**: 465–492.

Shade A, Handelsman J. 2012. Beyond the Venn diagram: the hunt for a core microbiome. *Environmental Microbiology* **14**: 4–12.

Shade A, Stopnisek N. 2019. Abundance-occupancy distributions to prioritize plant core microbiome membership. *Current Opinion in Microbiology* **49**: 50–58.

Singh BK, Nunan N, Ridgway KP, McNicol J, Young JPW, Daniell TJ, Prosser JI, Millard P. 2008. Relationship between assemblages of mycorrhizal fungi and bacteria on grass roots. *Environmental Microbiology* **10**: 534–541.

Staddon PL, Fitter AH, Graves JD. 1999. Effect of elevated atmospheric CO_2 on mycorrhizal colonization, external mycorrhizal hyphal production and phosphorus inflow in *Plantago lanceolata* and *Trifolium repens* in association

with the arbuscular mycorrhizal fungus *Glomus mosseae*. *Global Change Biology* **5**: 347–358.

Sun X, Chen W, Ivanov S, MacLean AM, Wight H, Ramaraj T, Mudge J, Harrison MJ, Fei Z. 2019. Genome and evolution of the arbuscular mycorrhizal fungus *Diversispora epigaea* (formerly *Glomus versiforme*) and its bacterial endosymbionts. *New Phytologist* **221**: 1556–1573.

Tabatabai MA, Bremner JM. 1969. Use of *p*-nitrophenyl phosphate for assay of soil phosphatase activity. *Soil Biology and Biochemistry* **1**: 301–307.

Tisserant E, Malbreil M, Kuo A, Kohler A, Symeonidi A, Balestrini R, Charron P, Duensing N, Frey NFD, Gianinazzi-Pearson V *et al.* 2013. Genome of an arbuscular mycorrhizal fungus provides insight into the oldest plant symbiosis. *Proceedings of the National Academy of Sciences, USA* **110**: 20117–20122.

Toju H, Peay KG, Yamamichi M, Narisawa K, Hiruma K, Naito K, Fukuda S, Ushio M, Nakaoka S, Onoda Y *et al.* 2018. Core microbiomes for sustainable agroecosystems. *Nature Plants* **4**: 247–257.

Trouvelot A, Kough JL, Gianinazzi-Pearson V. 1986. Mesure du taux de mycorhization VA d'un système radiculaire. Recherche de méthodes d'estimation ayant une signification fonctionnelle. In: Gianinazzi-Pearson V, Gianinazzi S, eds. *Physiological and genetical aspects of mycorrhizae*. Paris, France: INRA Press, 217–221.

Vandenkoornhuyse P, Baldauf SL, Leyval C, Straczek J, Young JPW. 2002. Extensive fungal diversity in plant roots. *Science* **295**: 2051.

Vandenkoornhuyse P, Quaiser A, Duhamel M, Le Van A, Dufresne A. 2015. The importance of the microbiome of the plant holobiont. *New Phytologist* **206**: 1196–1206.

Vannini C, Carpentieri A, Salvioli A, Novero M, Marsoni M, Testa L, de Pinto MC, Amoresano A, Ortolani F, Bracale M *et al.* 2016. An interdomain network: the endobacterium of a mycorrhizal fungus promotes antioxidative responses in both fungal and plant hosts. *New Phytologist* **211**: 265–275.

Walters WA, Jin Z, Youngblut N, Wallace JG, Sutter J, Zhang W, Gonzalez-Pena A, Peiffer J, Koren O, Shi Q *et al.* 2018. Large-scale replicated field study of maize rhizosphere identifies heritable microbes. *Proceedings of the National Academy of Sciences, USA* **115**: 7368–7373.

Wang F, Kertesz MA, Feng G. 2019. Phosphorus forms affect the hyphosphere bacterial community involved in soil organic phosphorus turnover. *Mycorrhiza* **29**: 351–362.

Wang F, Shi N, Jiang R, Zhang F, Feng G. 2016. *In situ* stable isotope probing of phosphate-solubilizing bacteria in the hyphosphere. *Journal of Experimental Botany* **67**: 1689–1701.

Yang W, Gu S, Xin Y, Bello A, Sun W, Xu X. 2018. Compost addition enhanced hyphal growth and sporulation of arbuscular mycorrhizal fungi without affecting their community composition in the soil. *Frontiers in Microbiology* **9**: 169.

Zhang K, Maltais-Landry G, George S, Grabau ZJ, Small IM, Wright D, Liao H-L. 2022. Long-term sod-based rotation promotes beneficial root microbiomes and increases crop productivity. *Biology and Fertility of Soils* **58**: 403–419.

Zhang L, Feng G, Declerck S. 2018a. Signal beyond nutrient, fructose, exuded by an arbuscular mycorrhizal fungus triggers phytate mineralization by a phosphate solubilizing bacterium. *ISME Journal* **12**: 2339–2351.

Zhang L, Peng Y, Zhou J, George TS, Feng G. 2020. Addition of fructose to the maize hyphosphere increases phosphatase activity by changing bacterial community structure. *Soil Biology and Biochemistry* **142**: 107724.

Zhang L, Shi N, Fan J, Wang F, George TS, Feng G. 2018b. Arbuscular mycorrhizal fungi stimulate organic phosphate mobilization associated with changing bacterial community structure under field conditions. *Environmental Microbiology* **20**: 2639–2651.

Zhang L, Xu M, Liu Y, Zhang F, Hodge A, Feng G. 2016. Carbon and phosphorus exchange may enable cooperation between an arbuscular mycorrhizal fungus and a phosphate-solubilizing bacterium. *New Phytologist* **210**: 1022–1032.

Zhang L, Zhou J, George TS, Limpens E, Feng G. 2022. Arbuscular mycorrhizal fungi conducting the hyphosphere bacterial orchestra. *Trends in Plant Science* **27**: 402–411.

Zhang S, Lehmann A, Zheng W, You Z, Rillig MC. 2019. Arbuscular mycorrhizal fungi increase grain yields: a meta-analysis. *New Phytologist* **222**: 543–555.

Zhou J, Chai X, Zhang L, George TS, Wang F, Feng G. 2020. Different arbuscular mycorrhizal fungi cocolonizing on a single plant root system recruit distinct microbiomes. *mSystems* **5**: e00929-20.

Supporting Information

Additional Supporting Information may be found online in the Supporting Information section at the end of the article.

Fig. S1 Details of the experimental sites and experimental system.

Fig. S2 Ratio of arbuscular mycorrhizal fungal to total fungal DNA copy number in hyphal samples across three sites.

Fig. S3 Rarefaction curve of operational taxonomic units for individual sample across the different datasets.

Fig. S4 Mycorrhizal colonization of host plants and hyphal length density in the in-growth tubes at each site.

Fig. S5 Correlation matrix (Spearman) of phosphatase activities and soil properties in the tubes across the three sites.

Fig. S6 Box plot showing Shannon–Wiener diversity indices and observed species indices for three communities (arbuscular mycorrhizal fungi, hyphosphere, and bulk soil bacteria).

Fig. S7 Bipartite networks display experimental site-sensitive operational taxonomic units in bulk soil and hyphosphere bacterial communities.

Fig. S8 Hyphosphere-specific enriched operational taxonomic units are largely conserved at the class levels across three experimental sites.

Fig. S9 Co-occurrence networks visualizing the significant pairwise correlations ($r > 0.8$; $P < 0.01$) between operational taxonomic unit pairs for bacteria in the hyphosphere, bacteria in the bulk soil, and arbuscular mycorrhizal fungi.

Fig. S10 16S rRNA gene copy number of the hyphosphere bacteria across three sites.

Fig. S11 Mycorrhizal colonization of host plants and hyphal length density in the hyphal compartments under each soil type in Experiment 2.

Fig. S12 Difference of phosphorus contents and phosphatase activities in the hyphal compartment inoculated or not inoculated with arbuscular mycorrhizal fungi in Experiment 2.

Fig. S13 Profiling of hyphosphere bacterial communities in Experiment 2.

Fig. S14 Qualitative taxonomic composition of module 4 (M4) in Experiment 1 and module 30 (M30) in Experiment 2 is reported as proportional operational taxonomic units numbers per class.

Methods S1 Details of the experimental setup.

Table S1 Physicochemical properties of the soil used in Experiments 1 and 2.

Table S2 Comparison between the hyphosphere core microbiome in our study and the root-associated core microbiome in previous studies.

Please note: Wiley is not responsible for the content or functionality of any Supporting Information supplied by the authors. Any queries (other than missing material) should be directed to the *New Phytologist* Central Office.

See also the Commentary on this article by Johnson & Marín, **238**: 461–463.